HARMO22
22nd International Conference on
Harmonisation within Atmospheric Dispersion Modelling for Regulatory Purposes
10-14 June 2024, Pärnu, Estonia

CFD MODELLING OF THE URBAN MICROCLIMATE: A PORTUGUESE CASE STUDY

Diogo Nascimento[1], Ana Ascenso[1], Ana Miranda[1], Myriam Lopes[1] and Vera Rodrigues[1]

[1]CESAM and Department of Environment and Planning, University of Aveiro, Portugal

Abstract: The urban microclimate plays a key factor in city living conditions. Understanding Urban Boundary Layer dynamics is crucial for enhancing urban planning and taking action for urban sustainability in a climate change context. This work focuses on CFD modelling a portion of the city of Aveiro and assessing the temperature patterns and the influence of near-wall temperatures on buoyancy during the peak hours of radiation during a heatwave.
Results show temperature variations across the area, supporting the identification of cooler areas and local hotspots. The findings inform urban planning strategies for mitigating extreme temperatures and fostering climate-resilient cities.

Keywords: *Temperature; Urban physics; OpenFOAM; Heatwave***.**

INTRODUCTION

Urban areas increasingly suffer from extreme weather events, which worsen the negative effects of the urban heat island effect and air pollution episodes (Pyrgou et al., 2020; Santamouris, 2020). In urban areas, high temperatures can cause the formation and spread of air pollutants. The heat accelerates chemical reactions that generate secondary pollutants, including ground-level ozone and secondary particulate matter. Moreover, low wind speeds during high heat periods can exacerbate air pollution buildup.
In recent years, Computational Fluid Dynamics (CFD) modelling has established itself as a powerful tool for studying the complex dynamics of urban microclimates. This approach allows for a full and detailed analysis of airflow patterns, temperature distributions, and pollutant dispersion within urban environments (Allegrini et al., 2014; Rodrigues et al., 2024).Some CFD methodologies still lack the full accountability of heat in their or the oversimplification of the temperature conditions (ex: solar radiation interactions) (Mirza et al., 2022; Mirzaei, 2021).

The present work presents CFD simulations that are performed for a heat-wave day accounting for material properties, heat exchanges between built environments and urban atmosphere and solar radiation interactions.

METHODOLOGY

A realistic urban domain scenario was developed and modelled to analyze microclimate dynamics during a high-temperature event. Specifically, July 17, 2020, was chosen as the interest period, representing the peak of a heatwave in Aveiro, Portugal.

The boundary conditions were obtained from the Weather Research & Forecasting Model (WRF) model for the target day were employed as the boundary conditions for the OpenFOAM model. Additional information regarding the WRF methodology, validation and results are available in Lopes et al. (2022).

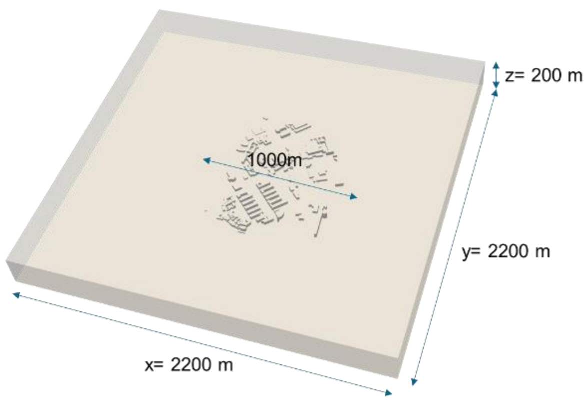

Figure 1. CFD computational domain.

Within OpenFOAM, the methodology utilizes the PIMPLE algorithm, a combination of PISO (Pressure Implicit with Splitting of Operator) and SIMPLE (Semi-Implicit Method for Pressure-Linked Equations). The modelling approach employs an Unsteady Reynolds-Averaged Navier–Stokes (URANS) methodology, incorporating a realizable k-ε turbulence model.

The computational domain is $2200\,m \times 2200\,m \times 200\,m$, as presented in Figure 1, with the tallest structure in the interest area reaching 40 m (H_{max}) in height. The domain was developed following the standard procedures outlined in Franke et al. (2007). Three unstructured domain meshes were constructed to assess grid independence. The obtained resolutions were: coarse (around 2.5M cells), medium (7M cells), and fine (12.5M cells). The coarse detail mesh was determined to possess resolution adequate for the outcomes presented in this study, with negligible disparities noted upon comparison with results derived from both the medium and fine meshes. Vertical logarithmic profiles were imposed as the inlet boundary conditions for horizontal wind speed (U), turbulence kinetic energy (k), and turbulent kinetic energy dissipation rates (ε).

Standard velocity and roughness wall functions were applied for the walls, while for the thermal behaviour of walls, a heat flux exchange wall function was utilized to consider both thermal and radiative interactions as in equation 1. With q being the the heat transfer rate $[W]$, R_{tot} the total thermal resistance $[KW^{-1}]$, A the area $[m^2]$, ΔT is the temperature difference $[K]$, T_s the surface total temperature $[K]$, T_{sur} the surrounding temperature $[K]$, ε the emissivity $[-]$ and σ the Stefan–Boltzmann constant $[Wm^{-2}K^{-4}]$. Solar radiation was modelled using OpenFOAM solar modules.

$$q = \left(\frac{1}{R_{tot}A}\,A\Delta T\right) + \varepsilon\sigma(T_s^4 - T_{sur}^4) \qquad (1)$$

There are multiple wall materials and surfaces in the domain area and these were grouped in essentially, six materials commonly found in the study area. The properties of the materials are presented in Table 1 (Bergman and Lavine, 2017; Oke et al., 2017).

Table 1. Domain materials/surface properties.

Material	Absorptivity (α)	Emissivity (ε)	Thermal conductivity (k)
Asphalt (middle-aged)	0.84	0.93	0.75
Red brick	0.60	0.92	0.83
Concrete wall	0.77	0.91	1.51
Limestone pavement	0.30	0.90	1.29
Water surfaces	0.75	0.95	0.57
Low vegetation surfaces	0.80	0.95	1.00

RESULTS AND DISCUSSION

The entire day was simulated, with results being saved every minute and then averaged every hour. In this section, we analyze the average temperature values between 14h and 15h. This hour was selected because it falls within the period of the highest accumulated heat in the area.

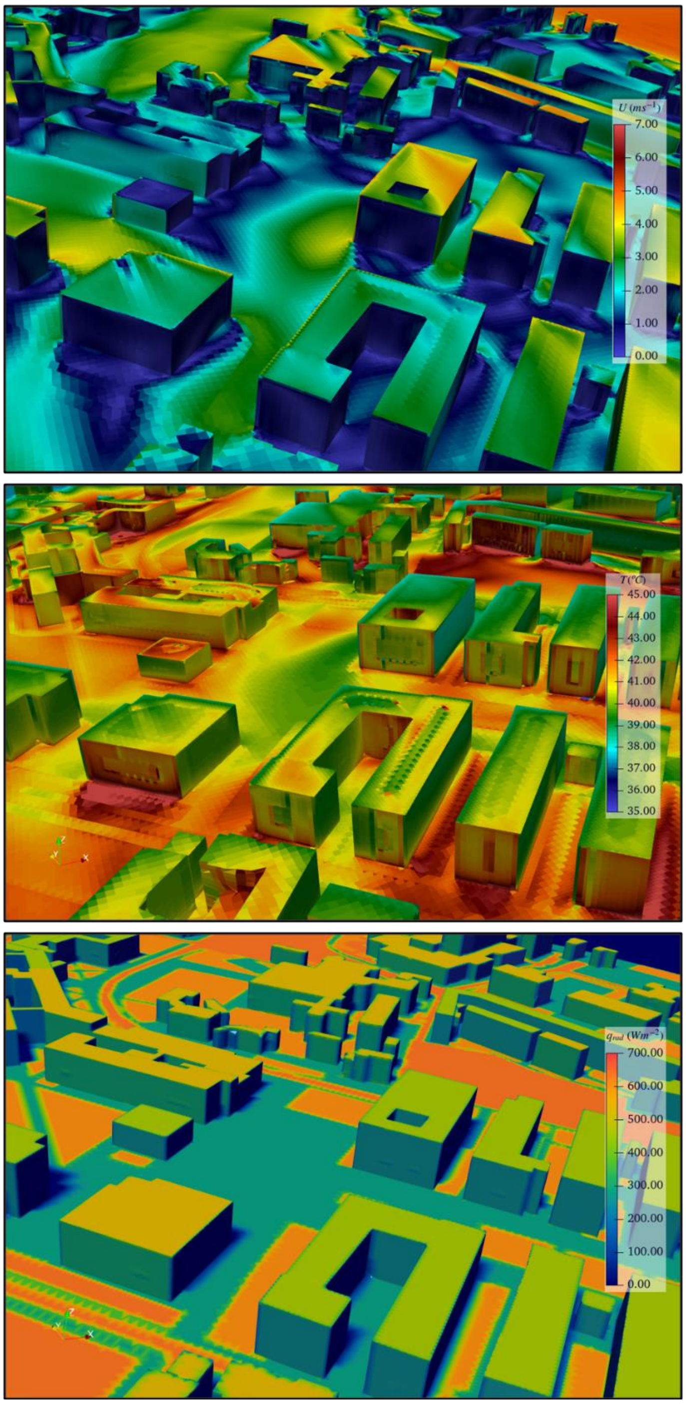

Figure 2. Averaged 14h-15h results for Wind Speed, Temperature and Radiative Heat Flux.

In Figure 2 we can observe the surface cells results and it is clear the locations where lower wind speeds occur in conjunction with higher solar radiation (radiative heat exchanges) we obtain a local increase in near-wall air temperature.

On the other hand, higher wind velocities promote cooler temperatures near the wall due to faster heat dissipation. Higher air temperatures occur within the cavity zone in the overall building wake region, closer to the ground where materials with higher absorptivity occur (asphalt) or in between buildings that are closer to each other with reduced spacing due to skimming flow that causes heat entrapment. The recorded maximum absolute temperatures for the day in the reference meteorological tower were of 37.8 $°C$. Analysing Figure 3, which exhibits the temperature in a horizontal plane at a height of 1.75 meters, we can see that near-wall air temperatures reach maximum values of 44.3 $°C$ and locations with minimum temperatures of 37.3 $°C$ with the overall area exhibiting a mean temperature value of 39.9 $°C$.

It is also visible here that the cavity region of the building wake experiences higher temperatures due to lower wind speeds.

It is worth noting that within the interest area, some green areas were considered as low vegetation surfaces based on their radiative and thermal properties. However, these areas do not necessarily promote the cooling effect that comes from the evaporation process, also trees were not accounted for in this study. Additionally, water surfaces were assumed to be flat surfaces with constant albedo and emissivity values. It is important to keep in mind that this assumption is not entirely representative of what happens in a real scenario.

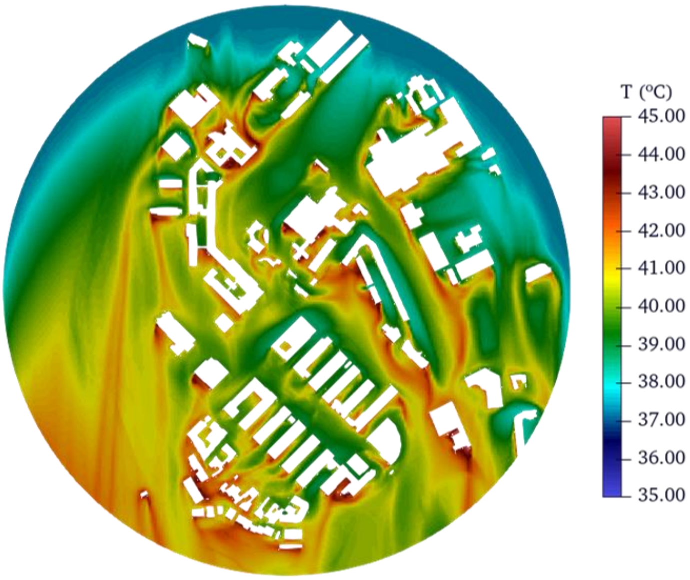

Figure 3. Temperature results for 14h-15h at 1.74 m high.

CONCLUSIONS

This study presents a 3D CFD simulation providing key insights into the complex dynamics of urban microclimates during a high-temperature event. The simulations highlight a methodology that accounts for material properties, heat exchanges, and solar radiation interactions for temperature distributions within urban environments. OpenFOAM results show that despite the maximum absolute air temperature recorded for the day, simulated near-wall air temperatures can reach higher values (up to 6.5 $°C$ of difference). Solar radiation and surface heat exchanges are key thermal interactions to assess the urban air temperature, with even more interest in low wind-speed locations. Furthermore, the developed module in this study will be essential when incorporating CFD simulations of the dispersion of pollutants in urban areas, accounting for distinct stability conditions – other than the neutral conditions typically used in CFD simulations at the microscale. Therefore, this study is very well aligned with the main theme of the Harmonisation conference, aiming to establish common frames of reference focusing on urban air quality modelling.

REFERENCES

Allegrini, J., Dorer, V., Carmeliet, J., 2014. Buoyant flows in street canyons: Validation of CFD simulations with wind tunnel measurements. Build Environ 72, 63–74. https://doi.org/10.1016/J.BUILDENV.2013.10.021

Bergman, T.L., Lavine, Adrienne.S., 2017. Fundamentals of Heat and Mass Transfer, 8th ed. John Wiley & Sons.

Franke, J., Hellsten, A., Schlünzen, H., Carissimo, B., 2007. COST Action 732: BEST PRACTICE GUIDELINE FOR THE CFD SIMULATION OF FLOWS IN THE URBAN ENVIRONMENT. Hamburg.

Lopes, D., Rafael, S., Ferreira, J., Relvas, H., Almeida, S.M., Faria, T., Martins, V., Diapouli, E., Manousakas, M., Vasilatou, V., Fetfatzis, P., Miranda, A.I., 2022. Assessing the levels of regulated metals in an urban area: A modelling and experimental approach. Atmos Environ 290, 119366. https://doi.org/10.1016/J.ATMOSENV.2022.119366

Mirza, S., Niwalkar, A., Anjum, S., Bherwani, H., Singh, A., Kumar, R., 2022. Studying impact of infrastructure development on urban microclimate: Integrated multiparameter analysis using OpenFOAM. Energy Nexus 6, 100060. https://doi.org/10.1016/j.nexus.2022.100060

Mirzaei, P.A., 2021. CFD modeling of micro and urban climates: Problems to be solved in the new decade. Sustain Cities Soc. https://doi.org/10.1016/j.scs.2021.102839

Oke, T.R., Mills, G., Christen, A., Voogt, J.A., 2017. Urban Climates. Cambridge University Press. https://doi.org/10.1017/9781139016476

Pyrgou, A., Hadjinicolaou, P., Santamouris, M., 2020. Urban-rural moisture contrast: Regulator of the urban heat island and heatwaves' synergy over a mediterranean city. Environ Res 182. https://doi.org/10.1016/j.envres.2019.109102

Rodrigues, V., Augusto, B., Oliveira, K., Ascenso, A., Rafael, S., Nascimento, D., Miranda, A.I., 2024. Setting up a CFD model to evaluate the impact of green infrastructures on local air quality. Air Qual Atmos Health. https://doi.org/https://doi.org/10.1007/s11869-024-01567-6

Santamouris, M., 2020. Recent progress on urban overheating and heat island research. Integrated assessment of the energy, environmental, vulnerability and health impact. Synergies with the global climate change. Energy Build. https://doi.org/10.1016/j.enbuild.2019.109482